

Article

Seasonal and Inter-Annual Variability of Groundwater and Their Responses to Climate Change and Human Activities in Arid and Desert Areas: A Case Study in Yaoba Oasis, Northwest China

Huanhuan Li ¹, Yudong Lu ^{1,*}, Ce Zheng ¹, Xiaonan Zhang ², Bao Zhou ³ and Jing Wu ³

¹ Key Laboratory of Subsurface Hydrology and Ecological Effects in Arid Region of Ministry of Education, School of Water and Environment, Chang'an University, Xi'an 710054, China; 17742499497@163.com (H.L.); ruudfanshd@139.com (C.Z.)

² Hanjiang Bureau of Hydrology and Water Resources Survey, Bureau of Hydrology, Changjiang Water Resources Commission, Xiangyang 441000, China; zhangzxn@163.com

³ Geological Environmental Monitoring Central Station of Qinghai Province, Xining 810001, China; zhb820322@163.com (B.Z.); endless5wj@163.com (J.W.)

* Correspondence: luyudong18@163.com; Tel.: +86-176-0298-3162

Received: 25 November 2019; Accepted: 16 January 2020; Published: 20 January 2020



Abstract: Climate change and human activities have profound effects on the characteristics of groundwater in arid oases. Analyzing the change of groundwater level and quantifying the contributions of influencing factors are essential for mastering the groundwater dynamic variation and providing scientific guidance for the rational utilization and management of groundwater resources. In this study, the characteristics and causes of groundwater level in an arid oasis of Northwest China were explored using the Mann–Kendall trend test, Morlet wavelet analysis, and principal component analysis. Results showed that the groundwater level every year exhibited tremendous regular characteristics with the seasonal exploitation. Meanwhile, the inter-annual groundwater level dropped continuously from 1982 to 2018, with a cumulative decline depth that exceeded 12 m, thereby causing the cone of depression. In addition, the monthly groundwater level had an evident cyclical variation on the two time scales of 17–35 and 7–15 months, and the main periodicity of monthly level was 12 months. Analysis results of the climatic factors from 1954 to 2018 observed a significant warming trend in temperature, an indistinctive increase in rainfall, an inconspicuous decrease in evaporation, and an insignificant reduction in relative humidity. The human factors such as exploitation amount, irrigated area, and population quantity rose substantially since the development of the oasis in the 1970s. In accordance with the quantitative calculation, human activities were decisive factors on groundwater level reduction, accounting for 87.79%. However, climate change, including rainfall and evaporation, which contributed to 12.21%, still had the driving force to change the groundwater level in the study area. The groundwater level of Yaoba Oasis has been greatly diminished and the ecological environment has deteriorated further due to the combined effect of climate change and human activities.

Keywords: climate change; human activity; principal component analysis; cone of depression; groundwater level; arid oasis

1. Introduction

Groundwater resources play a crucial role in social, economic, and agricultural development, particularly in arid and semi-arid regions where surface water is scarce [1–3]. It is not just the vital water

supply, but the basic conditions and determinant factors for the maintenance of desert ecosystems. In general, groundwater depletion has always been being the leading cause of ecological degradation in arid and semi-arid areas [4,5]. With the occurrence of global change, climate anomalies, and rapid development of the social economy in recent decades, the impacts of climate change and human activities on groundwater resource have been increasingly prominent in arid oases which are characterized by scarce surface water, intense human activities, atrocious climates, and fragile ecosystems [6,7]. According to previous research, the groundwater level has sharply declined as a combined result of natural and human factors and has subsequently triggered a series of eco-environmental problems in many arid oases of China. Keilholz et al. [8] observed serious aquifer depletion and environmental degradation occurred in the Tarim area. Abliz et al. [9] summarized the groundwater depth increase because of extensive agricultural water consumption and regional evapotranspiration in the Keriya Oasis, resulting in soil salinization and degradation downstream. Hao et al. [10] indicated the continuous declination in the groundwater resources of Minqin Oasis with long-term over-extraction. These wide-ranging consequences for ecosystems have not only been noticed in typical oases along the ancient Silk Road of Northwest China, but also reported in the arid and semi-arid regions of other countries, such as, India [11], Australia [12], the United States [13], Egypt [14], Morocco [15], and Central Asia [16].

Multiple climatic and human factors are generally intricate and difficult to distinguish. Therefore, many relevant studies have only addressed groundwater resources from the individual effect of either climate change [17,18] or human activities [19,20]. In recent years, more investigations have focused on groundwater resources responding to climate change coupled with human activities using integrated hydrological modeling, climate coefficient, sensitivity analysis, and quantitative evaluation methods. Keilholz et al. [8] used the MIKE System Hydrological European (MIKE SHE) integrated hydrological model to analyze the impacts of climate change and land use on groundwater and ecosystems of Tarim River. Russo et al. [21] explored the recent characteristics of groundwater level in deep aquifers across the USA and its response to decadal climate variability and pumping through geographical information system. Malekinezhad and Banadkooki simulated the groundwater level using a three-dimensional finite-difference model (MODFLOW) and developed the coupled model to analyze the influence of climate change and human pressures on it in Iran [22]. Wang et al. [23] assessed the combined effect of climate change and intensive human activities on the groundwater system of Guanzhong Basin (central China) based on an integrated approach of multivariate statistical analysis, wavelet analysis, and base flow index. Feng et al. [24] constructed an integrated hydrological modeling to attribute the climatic and human impacts on groundwater in North China Plain by using the groundwater and surface-water flow model (GSFLOW). As in the aforementioned cases, numerous studies have been conducted on groundwater and its influencing factors. Although some investigations had improved the understanding on the recharge and discharge physical processes in groundwater and how it responds to climate variation and human interference, research on the relative extent of influencing factors in arid regions has been rare and has made little progress so far. In conclusion, among the main issues with regard to the groundwater impacted by climate change and human activities exist the following aspects: (1) which indicators should be selected to evaluate, and (2) how to distinguish and quantify the proportion of impact factors.

In the current study, with Yaoba Oasis taken as the typical research region, the changes and major influencing factors of groundwater level from 1982 to 2018 were analyzed using the Mann–Kendall (MK) trend test, Morlet wavelet analysis, and principal component analysis (PCA). This work aimed to (1) evaluate the long-term variation characteristics of groundwater level, (2) study the mutation test and change trend of climate change and human activity, and (3) calculate the quantitative indicators of groundwater level response to climatic and human factors. The results can offer scientific references for the rational exploitation of groundwater resources, and help explore effective measures to handle climate change and human activities in the arid oasis.

2. Materials and Methods

2.1. Study Area and Data Source

Yaoba Oasis is the largest agricultural irrigation area of Alxa League in the Inner Mongolia Autonomous Region, which is a typical artificial desert oasis in northwest China accounting for an area of approximately 81.20 km² (Figure 1a). The study area is located at the edge of the diluvial sloping plain on Helan Mountain and its topography is controlled by four north-south spreading faults, ranging from high in the east and low in the west (Figure 1c). According to statistics, the study area has a mean annual temperature of 8.33 °C, an average annual precipitation as low as 201.95 mm, and an average annual evaporation as high as 2296.6 mm. In summary, Yaoba Oasis presents a typical continental arid climate with the following characteristics: intense evaporation, scarce precipitation, hot summer, and cold winter [25]. Groundwater resources play a crucial role in the local social development and agricultural production in Yaoba Oasis because of surface water shortage and rare precipitation in the area. The groundwater was mainly derived from the lateral rainfall recharge in the west side of Helan Mountain with the replenishment amount of 31 million throughout the year. The groundwater runoff generally flowed from northeast to southwest. The quaternary system aquifer was the main extraction zone of groundwater and its thickness reached 10–30 m, containing phreatic water of the first aquifer group and confined water of the second aquifer group. Since the oasis was developed in the 1970s, the groundwater level has been continuously dropping, with a cumulative decline depth over 10 m impacted by climate change and human activities, forming the cone of depression [26]. Subsequently, a series of eco-environmental problems caused by the decline of groundwater level has been observed, such as deterioration of groundwater chemistry, intrusion of groundwater by saltwater, and the aggravation of soil salinization. Cui et al. [27] conducted the fixed-point observation on the soil salinity and chemical components of groundwater, and quantitatively evaluated their characteristics in different periods through gray relational analysis in Yaoba Oasis. The investigation proved that the soil salinization was severe with the salinization rate of 72.7% and the correlation of mineral content, pH, and the main ion content of groundwater with of soil was high. All of these groundwater problems impacted agricultural production, social and economic development, and the lives of the local people.

The 1954–2018 data of climatic factors, namely, temperature, rainfall, evaporation, and relative humidity, are sourced from the local meteorological station (E: 105°36′12.12″; N: 38°30′25.74″; H: 1295 m), while the data of groundwater levels from 1982 to 2018 are obtained from the monitoring network (Figure 1b). Those six wells with the depth of 100 m are mainly monitored in the first and second aquifer group in the quaternary system. The ZB-01 well as an automatic monitoring well, collects the groundwater level at 8:00 am once a day; the levels are manually monitored every 5 days (1, 6, 11, 16, 21, and 26) in the other 5 wells. All continuous and complete data are collected from the local hydrographic bureau.

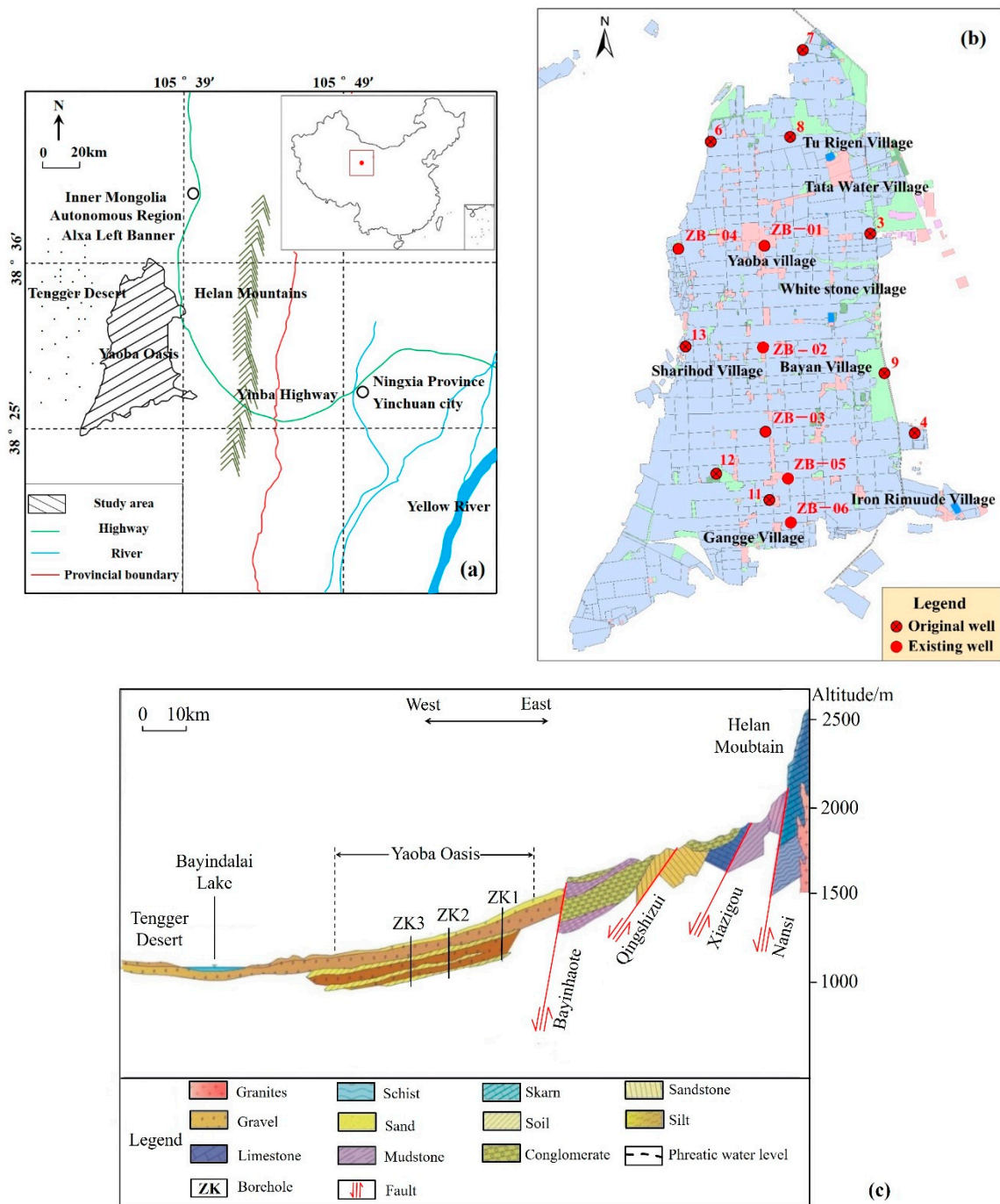


Figure 1. Map of the study region: (a) location map of Yaoba Oasis in Alxa Left Banner, Inner Mongolia Autonomous Region, China; (b) distribution of the monitoring wells of groundwater in Yaoba Oasis; (c) schematic of the geological section in Yaoba Oasis.

2.2. Research Methodology

The MK trend test was used to detect abrupt changes and the trends of climatic factors in this case study, which is a non-parametric statistical method based on rank correlation proposed by Mann in 1945 [28] and developed by Kendall in 1975 [29]. The test has a robust ability because it does not require the sample data to follow any specific distribution and is free from the disturbance of outliers [30]. Thereby, this trend test is widely used for the variation analysis of climatological variables over time. Polemio and Lonigro investigated the variations of monthly climatic time series (rainfall,

wet days, rainfall intensity, and temperature) and the annual maximum of short-duration rainfall [31]. Chowdhury et al. [32] evaluated the tendency and step changes in annual and seasonal rainfalls over more than 100 years in the South Australian region using MK test. Wu et al. [33] used the MK test to assess the trends in annual and seasonal rainfall since 1950s in Shaanxi Province of China. For details of the MK trend test we refer to Hamed [34] and Jia et al. [35].

This work next applied the wavelet analysis to identify the frequency characteristics and evolution trend of the monthly groundwater level. Wavelet transform is a more effective method than the Fourier transform to analyze multiple time scales of hydrological time series, which can truly reflect the periodicity of the given series and the distribution characteristics of the main cycles [36]. In particular, the discrete Morlet wavelet is simple to develop and requires less computation time for non-stationarity hydrological data such as rainfall [23], runoff [37] and groundwater [38,39]. The discrete form of the Morlet wavelet transform coefficient is defined as

$$W_f(a, b) = |a|^{-1/2} \Delta t \sum_{k=1}^N f(k\Delta t) \overline{\psi\left(\frac{k\Delta t - b}{a}\right)} \quad (1)$$

where Δt represents the time interval; a represents the scale factor reflecting the period wavelet; b represents the time factor indicating the shift in time domain; and $\psi(t)$ and $f(k\Delta t)$ represent the mother wavelet function and the discrete time series, respectively [40].

$W_f(a, b)$ in the 2D contour map can describe the data information in different time scales, phase, location, and intensity. In addition, the wavelet variance is calculated by Equation (2). The coefficient squares indicate the distribution and intensity of fluctuating energy at different time scales, which can determine the primary periods of hydrological time series [37].

$$Var(a) = \int_{-\infty}^{\infty} |W_f(a, b)|^2 db \quad (2)$$

The quantitative analysis between the influencing factors and groundwater is conducted at the end of the research based on the PCA method. PCA is a multivariate statistical method that can aggregate the impacts of multiple variables into few factors [41]. The basic idea of this technology is that the original variables are transformed into fewer variables through dimension reduction under the premise of loss of little information [42]. In other words, the new variable (principal component) can reflect the original information and is not repeated. PCA can replace the inter-correlated variables by the independent uncorrelated principal components to eliminate the effect of multicollinearity; given these abilities, it is widely applied in the field of groundwater resources (i.e., groundwater level [43], quality [44], and geochemistry [45]). The detailed principle and calculation steps are given in previous study [43].

3. Results and Discussion

3.1. Dynamic Characteristics of Annual Groundwater Level

With the monthly mean groundwater level from 1982 to 2018 of monitoring well ZB-02 in Yaoba Oasis taken as an example, the monthly average rainfall is found to be the most abundant from July to September, whereas the groundwater level is at the lowest phase of the whole year (Figure 2a). Hence, the rainfall does not change the overall trend of groundwater level during the year. Meanwhile, the monthly groundwater level is uncorrelated with monthly mean evaporation, temperature, and relative humidity to an extent by the qualitative analysis. Thus, the influence of climatic factors on the monthly groundwater level is negligible (Figure 2b–d). By contrast, the monthly groundwater level obviously drops as the monthly average exploitation quantity increases (Figure 2e). In other words, the variation of monthly groundwater level in the study area is opposite the change in monthly exploitation. Therefore, the annual groundwater level in Yaoba Oasis belongs to the dynamic exploitation type.

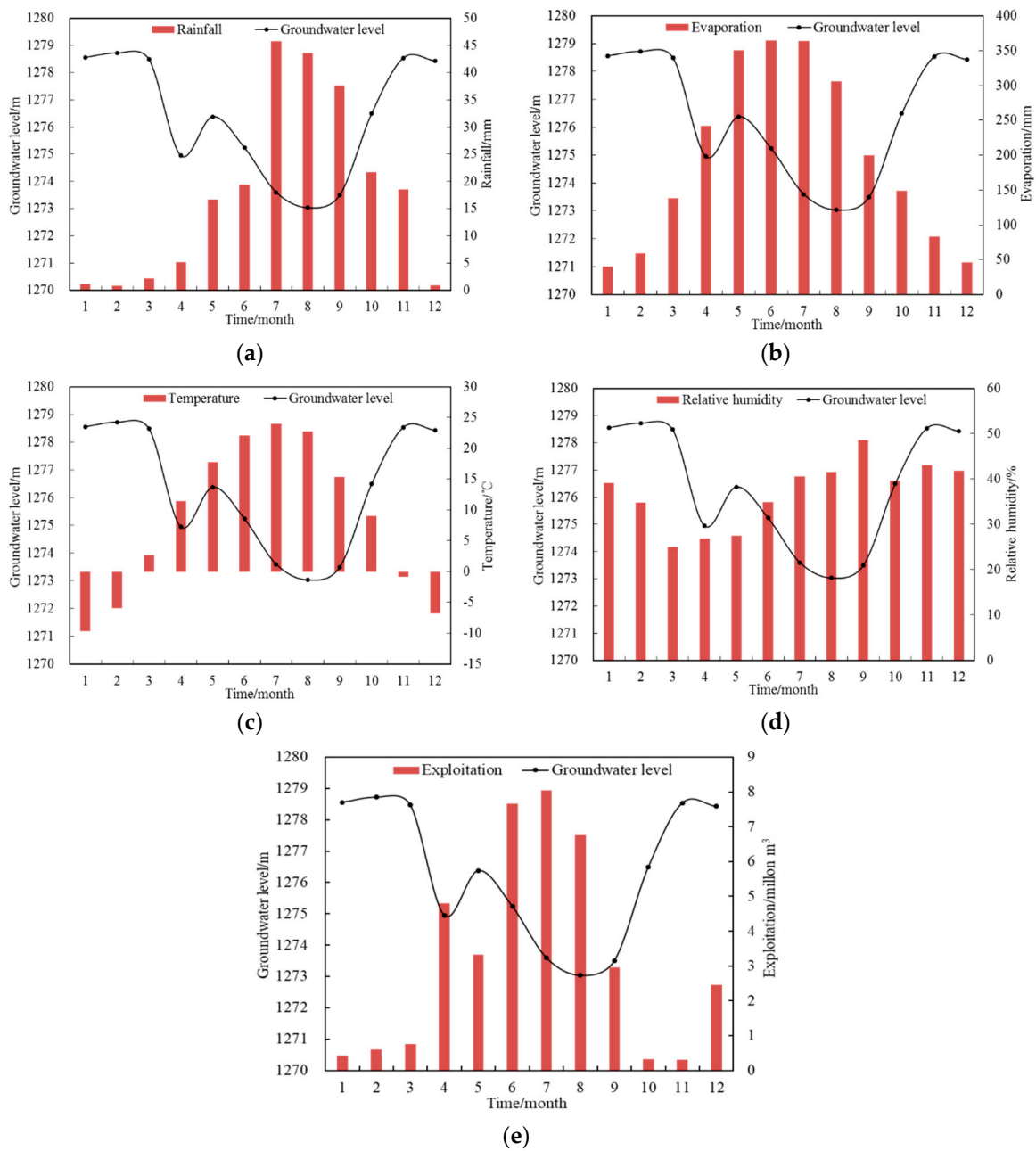


Figure 2. Contrast curves of the monthly average groundwater levels and influencing factors from 1982 to 2018 in the ZB-02 well. (a) Monthly groundwater level and rainfall; (b) monthly groundwater level and evaporation; (c) monthly groundwater level and temperature; (d) monthly groundwater level and relative humidity; (e) monthly groundwater level and exploitation.

As shown in Figure 3, the change fluctuation of monthly groundwater level in the ZB-01 well from 1982 to 2018 is low. The monitoring well lies in the living quarters where the domestic water for residents is supplied by the water supply company in the town. Thus, the exploitation quantity of groundwater is relatively few in the vicinity of the ZB-01 well. The variation curves of the other five monitoring wells are generally similar during the year and the monthly average groundwater level changes regularly as the seasonal exploitation amount varies in different seasons. As a result, the characteristic of annual groundwater level from 1982 to 2018 in the study area can be roughly summarized into four stages [27].

- (1) Intermittent irrigation period from January to February: The intensity of groundwater exploitation remains low, and the groundwater is only supplied for residents' domestic water. The groundwater level begins to rise slowly after the end of winter irrigation in the previous year, reaching the highest level of the year in March and tending to be basically stable. The increased amplitude of groundwater level of the six wells is 0.25–0.79 m from January to February.
- (2) Spring irrigation stage from March to May: The intensity of groundwater exploitation increases. Farmers begin large-scale cultivation and extract the groundwater for irrigating corn, sunflower, and millet. Groundwater level continues to drop to the lowest level in April, and the decline range is 0.06–1.35 m. The extraction intensity of groundwater is low due to the end of spring irrigation. The groundwater level gradually rises to 0.05–0.14 m during this stage.
- (3) Summer irrigation stage from June to August: This period lasts for the longest time and includes crop growth, which requires a large amount of groundwater to meet growth needs. The groundwater reaches the maximum intensity, and the exploitation quantity accounts for more than 65% of the whole year. The groundwater level drops rapidly to the lowest value of the year in August, forming a regional cone of depression, and the decline amplitude is 0.67–4.79 m at this period.
- (4) Intermittent irrigation stage from September to December: As the summer irrigation nears its end, exploitation intensity weakens. The groundwater exploitation remains at a low level during this period, and the groundwater level rises rapidly to 0.74–3.44 m. The increase in the rate of groundwater level fluctuates because of limited-scale winter irrigation. However, the overall trend continues to rise with the amplitude of 0.26–0.88 m from November to December.

The previous studies have indicated that the amount of groundwater recharge is maintained at approximately 31 million m³/year, while the total amount of exploitation is maintained at 40 million m³/year in Yaoba Oasis [46]. Although the groundwater level slowly recovers during the year, the recharge cannot still meet the exploitation, resulting in the gradual decline in groundwater level year after year. As a result, the groundwater level at the end of the year is always lower than that at the beginning of the year.

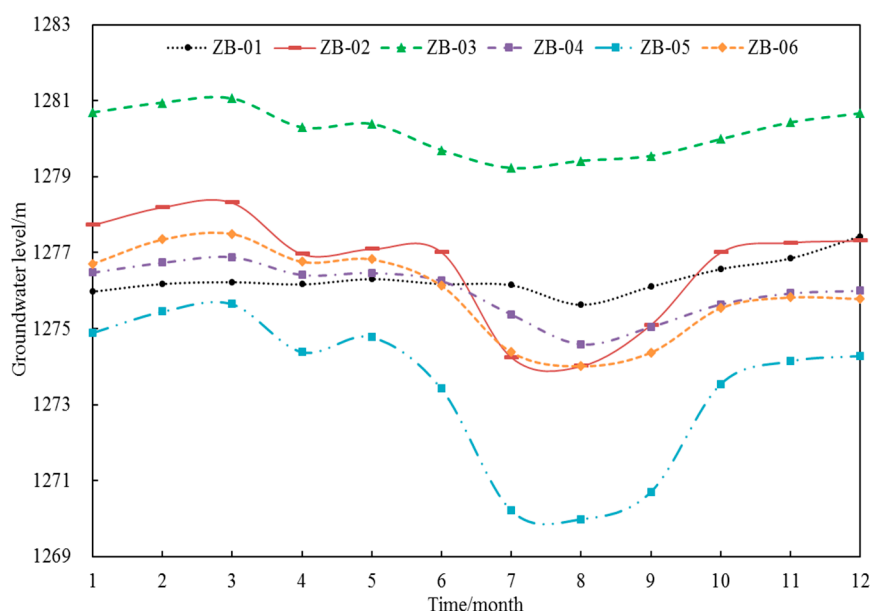


Figure 3. Variation curve of average monthly groundwater level from 1982 to 2018 in six monitoring wells.

3.2. Dynamic Characteristics of Inter-Annual Groundwater Level

3.2.1. Impact of Climatic Factors on Groundwater Level

(1) Trend of temperature

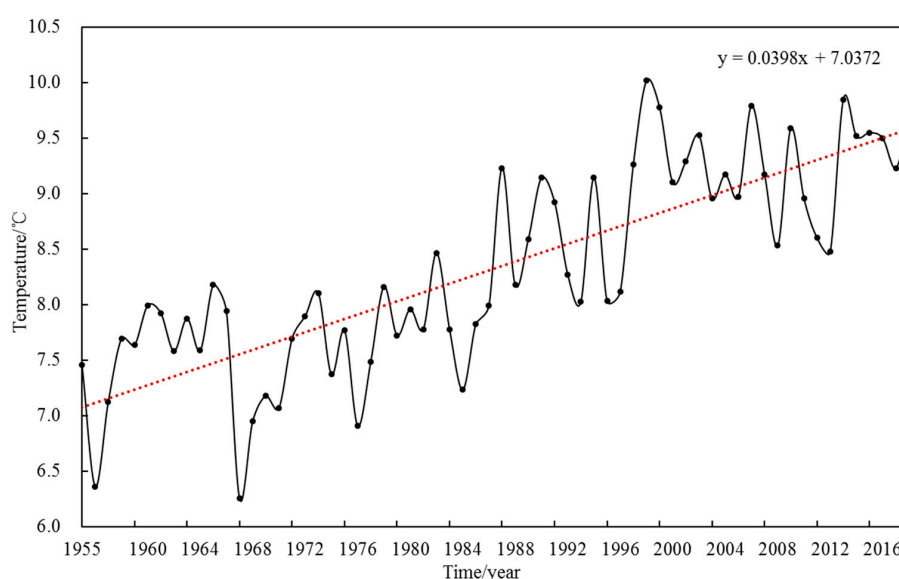
An analysis of the temperature data from 1955 to 2018 revealed that the average annual temperature in the study area was 8.33 °C, the lowest temperature was 6.25 °C in 1967, and the highest temperature was 10.02 °C in 1998. As shown in Figure 4a, the variability of inter-annual temperature exhibited a fluctuating rising trend, which was consistent with global warming. The trend equation of temperature was $y = 0.0398x + 7.0372$ ($R = 0.812$ **) using the linear trend analysis method, and the warming tendency indicated a decadal increasing rate of 0.398 °C (Table 1).

Table 1. Test results of linear trend analysis and Mann–Kendall (MK) trend test for climatic factors.

Climatic Factor	Temperature	Rainfall	Evaporation	Relative Humidity
Tendency rate	+0.0398 C/year	+0.8186 mm/year	−4.8801 mm/year	−0.1213%/year
R value	0.812 **	0.276 *	−0.599 **	−0.670 **
Mutation year	1986	1989, 2005, and 2009	2007	1980

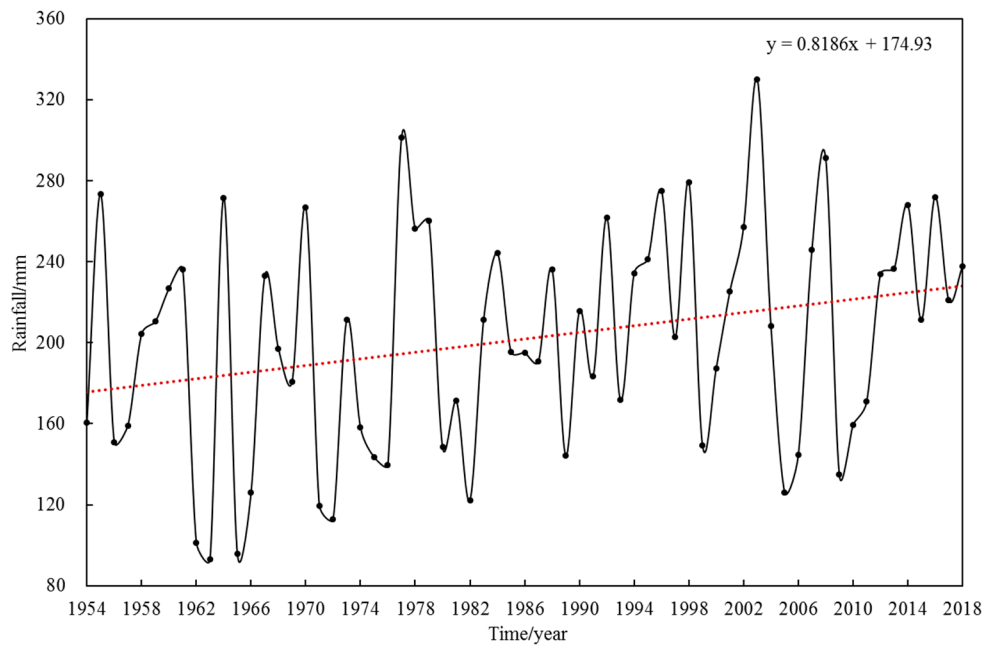
Note: * and ** mean passing the test at 0.05 and 0.01 significance level, respectively.

The MK trend test was used to test the mutation year of temperature for the 0.05 significance level and the ±1.96 critical lines [31]. Figure 5 clearly shows one intersection between the *UF* and *UB* curves, indicating that the mutation year of temperature occurred in 1986. Thus, the variability of annual temperature in the study area can be described as two stages: insignificant rise phase from 1955 to 1986 and significant rise phase from 1986 to 2018. The *UF* value was greater than 0 after 1955 and did not exceed the +1.96 critical line before 1986. That is, the temperature increased insignificantly during this period rising from 7.46 °C in 1955 to 7.99 °C in 1986. Next, the *UF* exceeded the +1.96 confidence interval after 1986. Thus, the temperature increased significantly rising from 7.99 °C in 1986 to 9.67 °C in 2018. The significant warming in temperature caused the irrigation water that was not absorbed by the crops to be consumed via evaporation, thereby causing drought in the farmland and increasing the irrigation times. This phenomenon further led to the increase in groundwater exploitation and the aggravation of soil salinization in the Yaoba Oasis.

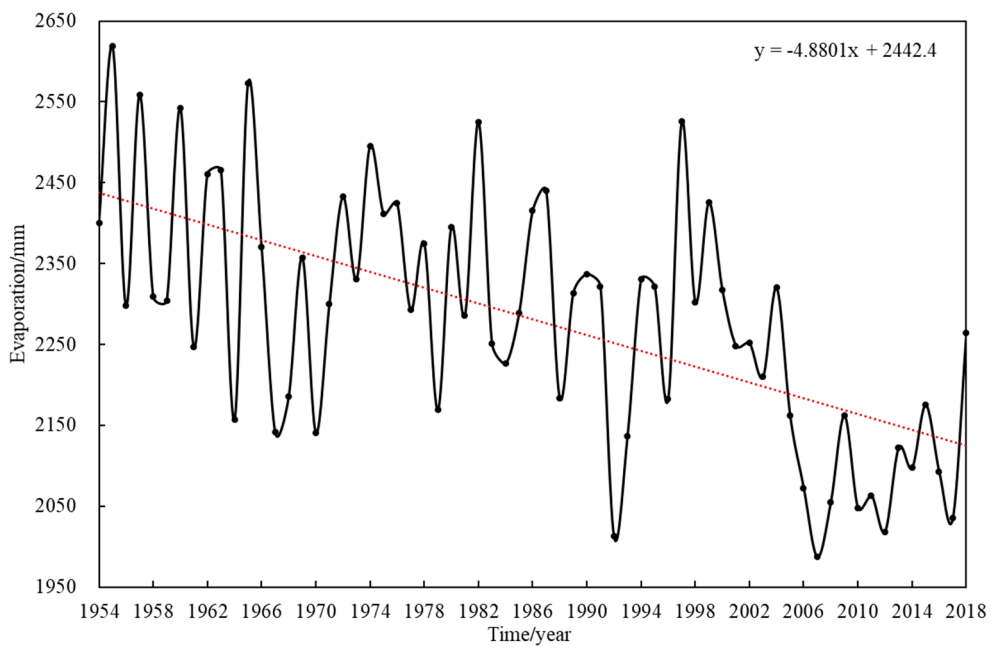


(a)

Figure 4. Cont.

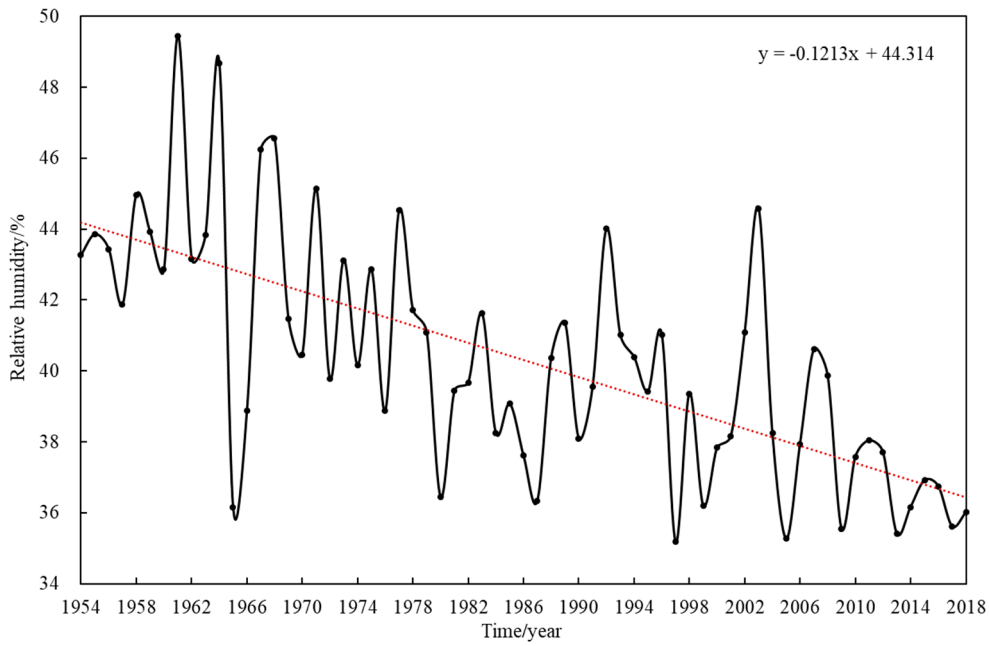


(b)



(c)

Figure 4. Cont.



(d)

Figure 4. Time series curve of climatic factors from 1954 to 2018. (a) Temperature from 1955 to 2018; (b) rainfall from 1954 to 2018; (c) evaporation from 1954 to 2018; (d) relative humidity from 1954 to 2018.

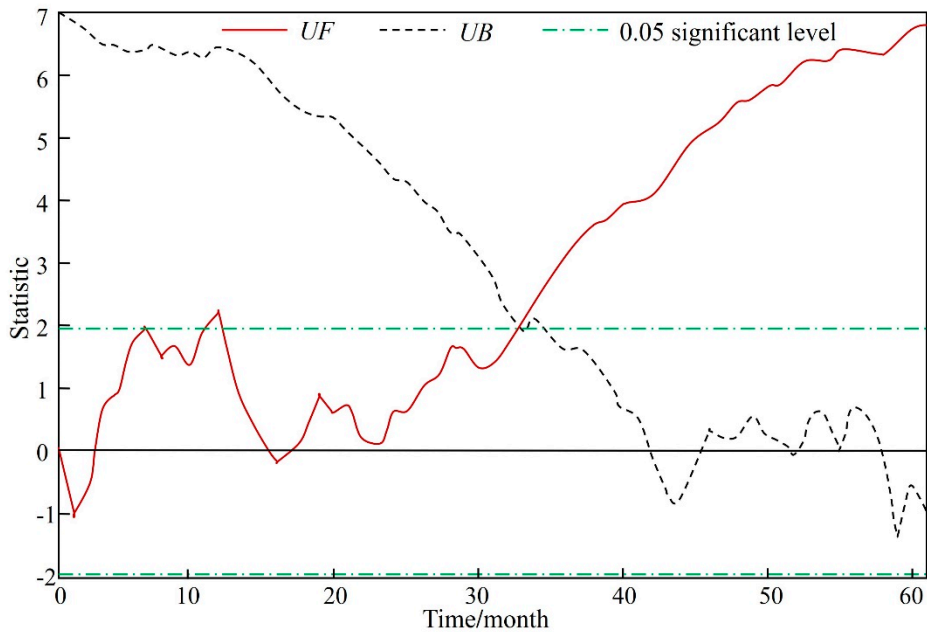


Figure 5. MK trend test curve of temperature from 1955 to 2018.

(2) Trend of rainfall

The average annual rainfall of the study area was 201.95 mm, minimum annual rainfall was 93.2 mm in 1963, and maximum annual rainfall was 330.1 mm in 2003 according to an analysis of rainfall data from 1954 to 2018. As shown in Figure 4b, the annual variation of rainfall greatly fluctuated with the trend equation of $y = 0.8186x + 174.93$. The increasing rate of rainfall was $+0.8186$ mm/year and $R = 0.276^*$. Three crossing points between *UF* and *UB* are listed in Table 1, and the mutation years of rainfall were 1989, 2005, and 2009, respectively. In accordance with the rainfall data from 1954 to

2018, the two points of 2005 and 2009 were mutation camouflage points, which were removed. Thus, the rainfall variation could be divided into two stages: insignificant reduction period from 1954 to 1989 and insignificant increase period from 1989 to 2018. The UF was less than 0, but it did not exceed the -1.96 critical line before 1989. Therefore, the rainfall trend had an insignificant decreasing fluctuation from 160.71 mm in 1954 to 144.32 mm in 1989. The UF was greater than 0, but it did not exceed the $+1.96$ critical line after 1989. Hence, the increasing trend was insignificant, rising from 144.32 mm in 1989 to 237.6 mm in 2018. Rainfall is not only an essential element of the water cycle in the arid oasis but also an important recharge source for groundwater. It recharges groundwater by means of surface infiltration replenishment. Therefore, following the rule of rainfall change and using seasonal flood to regulate groundwater resources are feasible methods.

(3) Trend of evaporation

The average annual evaporation was 2281.37 mm (11 times the precipitation) as calculated from the evaporation data from 1954 to 2018, and the minimum and maximum evaporation were 1987.09 mm in 2007 and 2618.70 mm in 1955, respectively. Figure 4c illustrates that the annual evaporation presented a fluctuant dropping tendency and that the trend equation was $y = -4.8801x + 2442.4$. The decreasing rate was -4.8801 mm/year and $R = -0.599^{**}$ (Table 1). The intersection between the UF and UB reflected the mutation year, that is, 2007. Thus, the evaporation change consisted of two phases: long-term insignificant reduction from 1954 to 2007 and short-term insignificant increase from 2007 to 2018. The UF was less than 0 after 1954, but it did not exceed the -1.96 critical line before 2007, indicating that the evaporation had an insignificant decline during this period, which decreased from 2400.7 mm in 1954 to 1987.09 mm in 2007. The UF then became greater than 0 but did not exceed the $+1.96$ critical line. Hence, the evaporation showed an insignificant increase afterwards from 1987.09 mm in 2007 to 2264.72 mm in 2018. According to previous research results, the intense evaporation in the arid region mostly exhausted the flood formed during the rainstorm season before it infiltrated into the groundwater [16,47]. In addition, water diversion and irrigation during the agricultural production increased the groundwater level and caused it to exceed the critical depth, resulting in continuous strong water evaporation in the shallow phreatic water area of the western part of study region, which worsened soil salinization [27,48,49].

(4) Trend of relative humidity

The average relative humidity was 40.34%, with minimum and maximum values of 35.18% in 1997 and 49.45% in 1961, respectively. Figure 4d shows that relative humidity declined from 1954 to 2018. The trend equation was $y = -0.1213x + 44.314$, dropping rate was -0.1213% /year, and $R = -0.670^{**}$ (Table 1). The intersection between UF and UB reflected that 1980 was the mutation year. The annual relative humidity could be divided into two stages: significant decreasing phase from 1954 to 1980, and insignificant decreasing phase from 1980 to 2018. The UF was less than 0, and it exceeded the -1.96 critical line after 1954. Hence, the relative humidity significantly decreased during this period from 43.27% in 1954 to 36.45% in 1980. The UF was less than 0, but it did not exceed the -1.96 critical line after 1980. Therefore, the relative humidity insignificantly declined from 36.45% in 1980 to 36.01% in 2018. The long-time reduction in relative humidity exacerbated the drought, resulting in increased groundwater extraction in the study area, which would cause a further decline in groundwater levels.

3.2.2. Impact of Human Activities on Groundwater Level

The impact of human activities on groundwater level dynamics in Yaoba Oasis is reflected by exploitation quantity, which is adjusted by the change in irrigated area, population, planting structure, and water-saving irrigation technology [26]. Taking the monitoring well ZB-02 as an example, the groundwater level in the non-irrigation (March) and irrigation (July) periods from 1982 to 2008 roughly declined as the exploitation quantity increased as evidenced in Figure 6. Then the groundwater level in March stabilized in the stage after 2008, whereas the groundwater level in July recovered after 2008.

The groundwater level of the ZB-02 well in July slowly decreased from 1287.59 m in 1982 to 1283.57 m in 1997 with a decline rate of 0.25 m/year. Subsequently, the groundwater level rapidly dropped to 1274.96 m in 2004 with a decline rate of 1.08 m/year. Afterwards, the descent of groundwater level gradually slowed down, and the level fell to the lowest value at 1273.63 m in 2008 with a decline rate of 0.27 m/year. The cumulative decline depth of 13.96 m occurred from 1982 to 2008. Drastic water-saving measures were implemented by the government to reduce the exploitation amount of groundwater in 2009. Thus, the groundwater level in July rebounded slightly to 1275.28 m in 2018 with a cumulative increase depth of 1.65 m and a rate of 0.165 m/year. During the short-term increasing period of groundwater level in the irrigation period, groundwater resources developed in a benign cycle in Yaoba Oasis. In fact, the rising trend of groundwater level in the non-irrigation period was not evident after 2009 and was basically in a stable phase. Given that no large-scale exploitation activities occurred in March, the groundwater level was a relatively static. Therefore, the monitoring data in the non-irrigation period could well reflect the change characteristic of groundwater level in the study area. The groundwater level in Yaoba Oasis gradually dropped as the exploitation quantity increased from 1982 to 2008 and then stabilized after 2008.

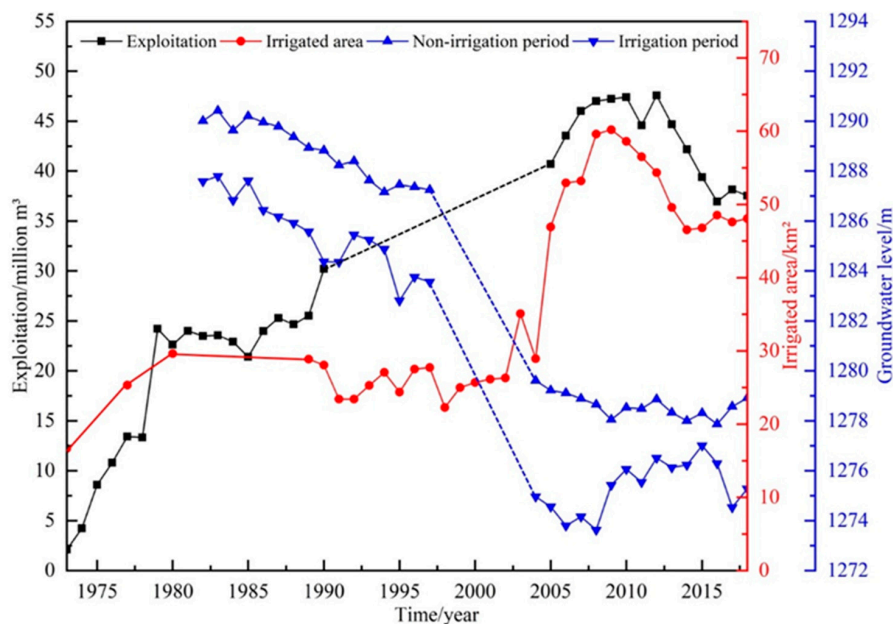


Figure 6. Variation curves of groundwater level in the non-irrigation (March) and irrigation (July) of the monitoring well ZB-02, exploitation quantity, and irrigated area from 1973 to 2018 (the dotted line refers to missing data.).

The variation characteristics of groundwater level in the six monitoring wells are summarized in Table 2. The other five wells showed the same variation law as the ZB-02 well. As a result, the inter-annual change in groundwater level in Yaoba Oasis affected by the exploitation amount can be roughly concluded as the following stages.

- (1) Slowly dropping period from 1981 to 1997: In the 1960s, the irrigated area was only 2.40 km², the amount of groundwater exploitation was only 1 million m³/year, and the depth of groundwater level was shallow. In 1973, agriculture began to rise rapidly with an irrigated area of 16.67 km² (Figure 6). This rise caused the exploitation quantity to increase sharply to 2.10 million m³/year. The irrigated area increased to 25.33 km² in 1977 with an exploitation amount of 13.43 million m³/year due to the continuous influx of migrants and the expansion of land. However, the groundwater level was generally stable because the recharge of 22 million m³/year was greater than the exploitation quantity. The irrigated area then rose to 29.33 km² in 1979, and the exploitation increased to 24.21 million m³/year. The exploitation amount was slightly larger

than the recharge. Therefore, the groundwater level slowly declined. In that year, the local government established the dynamic monitoring network because of the decline in groundwater (Figure 1c). Afterwards, the irrigated area was maintained at approximately 29.33 km², and the exploitation ranged from 23 million m³/year to 30 million m³/year, resulting in the continuous decline in groundwater level. The cumulative decline varied from 2.92 m to 4.64 m, and the rate was 0.17–0.27 m/year.

- (2) Rapidly declining period from 1997 to 2004: The irrigated area was stable at about 26.67 km². The crops were mostly water-consuming crops, such as corn and wheat, due to the unreasonable planting structure [25]. The amount of exploitation rapidly increased to around 40 million m³/year, causing a sharp drop of groundwater level. The cumulative decline was 1.95–9.33 m, and the rate of decline was 0.24–1.17 m/year.
- (3) Slowly declining period from 2004 to 2008: The irrigated area sharply increased from 28.93 km² in 2004 to 59.60 km² in 2008. The exploitation was maintained at 47 million m³/year, which far exceeded the recharge of 22 million m³/year. The cumulative depth of decline in five years was 0.2–1.5 m with a rate of 0.04–0.30 m/year.
- (4) Stable period from 2008 to 2018: The continuous drop of groundwater level attracted the attention of the local government in 2009. In recent years, water-saving measures had been taken in the study area. The irrigated area gradually reduced to 46.67 km², where the area of water-saving crops increased, and the planting proportion of water-consuming crops was relatively reduced. The exploitation amount was controlled at about 40 million m³/year, and the groundwater level was basically stable with a cumulative decline from –0.83 to 1.15 m and a descending rate of –0.08–0.12 m/year. In particular, the groundwater level of three monitoring wells rebounded slightly compared with the level in 2008. The irrigated area increased after 2014, but the exploitation was still declining. Thus, the quota water distribution system and planting structure improved by the government achieved remarkable results.

Therefore, the reduction of exploitation quantity plays a positive role in controlling the decline in groundwater level. To reduce the exploitation amount of groundwater resources, the implementation of water-saving irrigation technology, adjustment of agricultural planting structure, contraction of irrigated area, and other methods should be considered.

Table 2. Variation of groundwater level in six monitoring wells from 1981 to 2018.

Monitoring Year	Monitoring Well	Range of Groundwater Level (m)	Decline Amplitude (m)	Decline Rate (m)	Location
1981~1997	ZB-01	1285.77–1282.04	3.73	0.22	North-central
	ZB-02	1289.29–1286.03	3.25	0.20	Central
	ZB-03	1291.62–1288.70	2.92	0.17	South-central
	ZB-04	1284.47–1279.82	4.64	0.27	West-central
1997~2004	ZB-01	1282.04–1279.04	3.01	0.38	North-central
	ZB-02	1286.03–1278.43	7.60	0.95	Central
	ZB-03	1288.70–1279.37	9.33	1.17	South-central
	ZB-04	1279.82–1277.87	1.95	0.24	West-central
2004~2008	ZB-01	1279.04–1278.10	0.94	0.19	North-central
	ZB-02	1278.43–1276.93	1.50	0.30	Central
	ZB-03	1279.37–1278.25	1.12	0.22	South-central
	ZB-04	1277.87–1277.23	0.64	0.13	West-central
	ZB-05	1274.55–1273.50	1.05	0.21	South
	ZB-06	1276.02–1275.82	0.20	0.04	South
2008~2018	ZB-01	1278.10–1276.94	1.15	0.12	North-central
	ZB-02	1276.93–1277.27	–0.34	–0.03	Central
	ZB-03	1278.25–1279.08	–0.83	–0.08	South-central
	ZB-04	1277.23–1276.30	0.93	0.09	West-central
	ZB-05	1273.50–1274.05	–0.55	–0.06	South
	ZB-06	1275.82–1274.92	0.90	0.09	South

3.2.3. Variation of Cone of Depression

The large-scale development of groundwater resources has been conducted in the study area since 1978. With the continuous overexploitation of groundwater, unbalanced extraction has destroyed the natural runoff field of groundwater, resulting in the formation of a regional cone of depression. Figure 7a–c clearly present that the cone of depression of groundwater level has changed from the emergence phase to the expansion phase to the recovery phase. (1) The emergence phase: As the decline rate of groundwater level in the east was greater than that in the west, the single local cone of depression had a prototype in the east in July 1985 with the groundwater level in the center of cone of depression at 1280.42 m (Table 3). (2) The expansion phase: With the rapid development of agricultural resources, large-scale overexploitation caused the groundwater level to sharply decline. The center of cone of depression began to move westward, and the radius gradually expanded. The large cone of depression reached the middle of Yaoba Oasis in 2008 and formed a series of few-scale cone of depression in some areas. The groundwater level in the center of the biggest cone of depression was 1267.63 m, and the area of cone of depression expanded from 1.13 km² in 1985 to 27.16 km² in 2008. (3) The recovery phase: Under the influence of a series of water-saving measures after 2009, the range of the cone of depression reduced to 11.26 km². The center groundwater level increased from 1267.63 m in 2008 to 1274.26 m in 2018. Although the decline rate of groundwater level slowed significantly, and even the level of individual monitoring wells recovered from the historical minimum, the groundwater system still remained in over-exploitation status at this stage in the study area.

The difference in the cone of depression during the year was reflected in flow rate and area by comparing Figure 7c with Figure 7d. The shape of a cone of depression in the irrigation period was almost the same as that in the non-irrigation period, whilst the flow rate and direction of groundwater runoff had obviously changed. During the irrigation period in July, the variation in groundwater level was more complicated than that during the non-irrigation period in March. In particular, the center of the cone of depression was located in the strong extraction area with a central level of 1274.26 m, which mainly occurred in the middle and eastern parts of study area. The groundwater runoff flowed from the periphery to the center of cone of depression with a hydraulic gradient of approximately 1.91–8.30‰. Subsequently, the flow rate of groundwater runoff decreased to 0.0245–0.168 m/day and the hydraulic gradient diminished to approximately 6.7‰ as the end of the irrigation period. The groundwater level was gradually recovered and stabilized in March of the following year with a central level of 1276.59 m. Meanwhile, the range of the cone of depression was significantly fewer than that during the irrigation period shrinking from 11.26 km² in July to 9.84 km² in March and the diminutive cone of depression in some areas began to disappear.

Table 3. Characteristics of the cone of depression in groundwater level.

Location	Aquifer Group	Monitoring Month	Area of Cone of Depression (km ²)	Form	Central Groundwater Level (m)
East	Q ₂₊₃	1985/7	1.13	Mussel shape	1280.42
Central	Q ₂₊₃	2008/7	27.16	Oval shape	1267.63
Central	Q ₂₊₃	2018/7	11.26	Mussel shape	1274.26
Central	Q ₂₊₃	2018/3	9.84	Mussel shape	1276.59

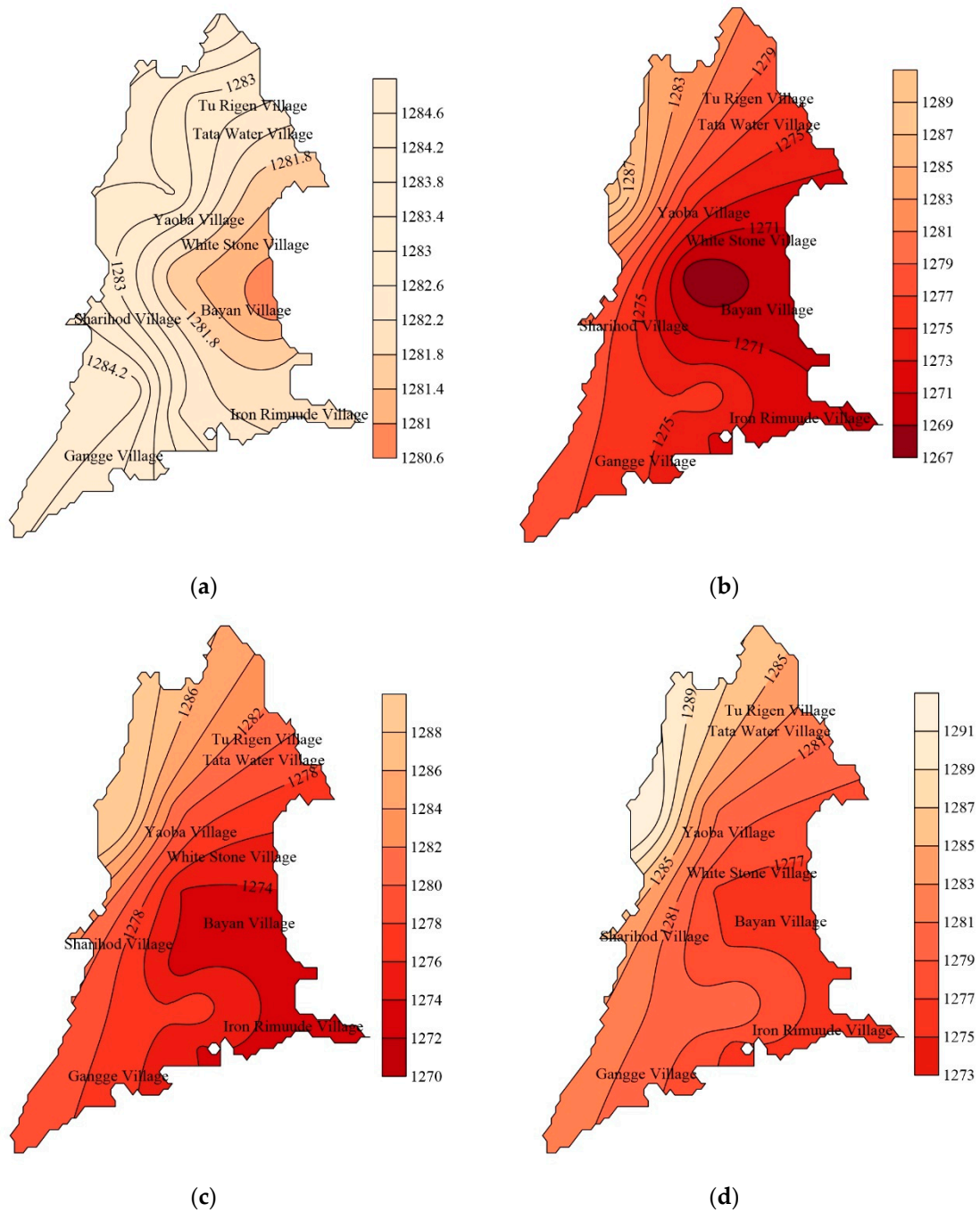


Figure 7. Contour map of groundwater level from 1985 to 2018. (a) July 1985 (irrigation period); (b) July 2008 (irrigation period); (c) July 2018 (irrigation period); (d) March 2018 (non-irrigation period).

3.3. Periodic Evolution Characteristics of Groundwater Level

In this work, Morlet wavelet transform was used to analyze the periodicity of the change in monthly groundwater level and the variation tendency of short-term seasonal groundwater level in the six monitoring wells from January 2010 to December 2018. The 2D isogram of the wavelet coefficient can visually present the signal strength of different time scales. The positive and negative changes in contour can further reflect the evolution and abrupt characteristics of the given sequence in near future. The positive value of the contour is represented by a solid line corresponding to the rise phase of the time series. By contrast, the negative value in the isogram is enclosed by a dashed line indicating the reduction phase [50]. As shown in Figure 8, the periodicity of monthly groundwater level in the

monitoring well ZB-04 had two evident time scales of 20–35 and 7–15 months. The phase structure of the two scales had a strong periodicity, and the positive/negative phase evenly fluctuated. The time scale from 20 to 35 months had four quasi-periodic oscillations with alternating high and low values. The positive phase of each period indicated that the groundwater level rose from January 2010 to February 2011, from March 2012 to April 2013, from May 2014 to June 2015, and from July 2016 to August 2017. In those rising periods, the four oscillation centers were distributed in August 2010, October 2012, November 2014, and February 2017, respectively. By contrast, the negative phase of each period meant that the groundwater level dropped from February 2011 to March 2012, April 2013 to May 2014, from June 2015 to July 2016, and from August 2017 to September 2018. During those declining periods, the four oscillation centers were distributed in July 2011, November 2013, January 2016, and March 2018, respectively. After September 2018, the contour of positive phase did not completely close. Thus, the rise of groundwater level occurred in the next few months. The time scale from 7 to 15 months had nine quasi-periodic oscillations with alternating high and low values. On the fewer time scales, the phase structure of groundwater level changed more frequently but became more chaotic and unstable than that on the larger time scales. Furthermore, the few and the large time scales nest each other. Thereby, the groundwater level of the ZB-04 well from January 2010 to December 2018 exhibited these time scales of 20–35 months and 7–15 months.

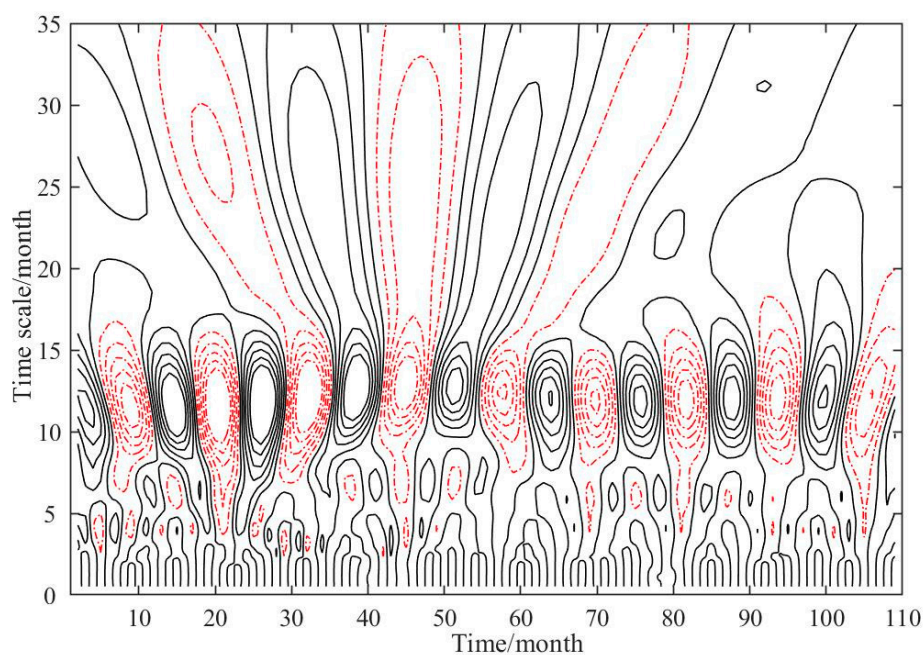


Figure 8. Time-frequency distribution of the real part of the wavelet coefficient.

The wavelet variance change in time scales was calculated using Equation (2) (Figure 9). As shown in the figure, the groundwater level of the ZB-04 well had two distinct peaks on the 12 months and 25 months scales. The 12 months corresponded to the maximum peak, indicating that the strongest oscillation occurred in this time scale, which was the first primary period of groundwater level. Therefore, the first and second main periods of groundwater level included 12 and 25 months, respectively. The above two main periods controlled the periodical evolution of groundwater level in the ZB-04 well from January 2010 to December 2018.

On the time scale of 20–35 months, the groundwater level was predicted to be in the rising period from September 2018 to October 2019 and from November 2020 to December 2021 and be in the dropping period from October 2019 to November 2020. On the time scale of 7–15 months, the groundwater level was predicted to be in the dropping period from August 2019 to March 2020 and in the rising period from March 2020 to August 2020. The oscillation intensity of the first main cycle was

much higher than that of the second main cycle. Thus, the prediction of the groundwater level on the 7–15 months scale was more accurate. Thereby, the periodicity characteristics of the groundwater level is once a year, and the groundwater level will drop from August to November and rise from December to May every year. As a result, the periodicity characteristics of 12 months calculated by the wavelet variance coincide with the annual variation of groundwater level in Section 3.1.

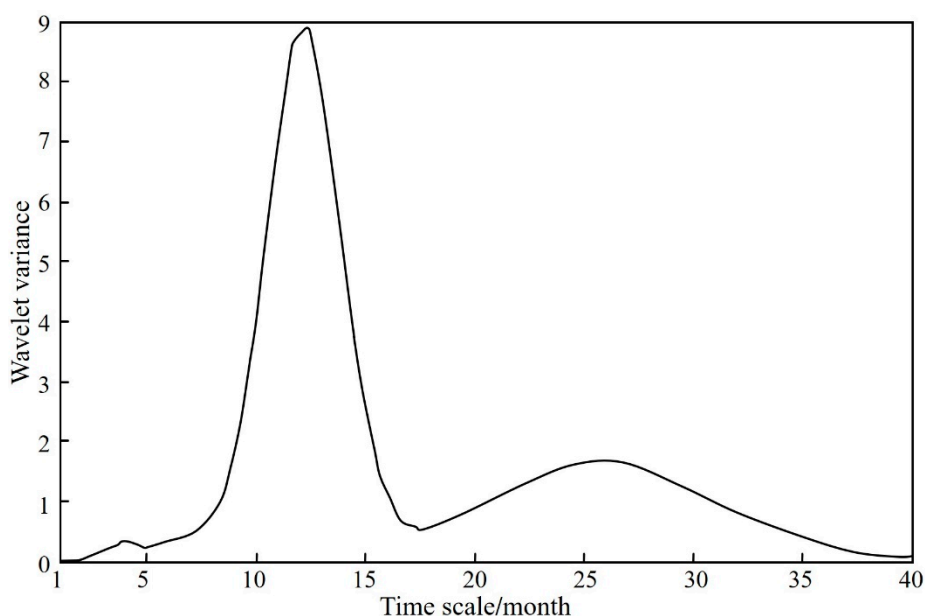


Figure 9. Wavelet variance curve of groundwater level.

The wavelet analysis results of periodic change in groundwater level in the six monitoring wells are listed in Table 4. Differences in the periodic variation of groundwater level in the six monitoring wells from January 2010 to December 2018 were consistent and subtle. The groundwater level had almost the same multi-time scales in the phase structure, containing the time scale of 7–15 months and the first primary period of 12 months. The variation of groundwater level in the six wells affected by climatic and human factors had evident periodicity of one year and synchronization. The groundwater level in the study area also had the dominant seasonal characteristics during the year. Therefore, the prediction results showed that groundwater level will be in the declining stage from March to August and will enter the recovery stage from September to February every year.

Table 4. Periodic characteristics of groundwater level in six monitoring wells.

Monitoring Well	ZB-01	ZB-02	ZB-03
Main Periodicity	12, 20 months	12, 22 months	12 months
Periodic Evolution of Different Time Scales	17–35 months, 4 times; 7–15 months, 9 times	17–35 months, 4 times; 7–15 months, 9 times	20–35 months, 4 times; 7–15 months, 9 times
Monitoring Well	ZB-04	ZB-05	ZB-06
Main Periodicity	12, 25 months	12, 21 months	12, 20 months
Periodic Evolution of Different Time Scales	20–35 months, 4 times; 7–15 months, 9 times	17–35 months, 4 times; 7–15 months, 9 times	20–40 months, 4 times; 7–15 months, 9 times

3.4. Quantitative Analysis of Major Influencing Factors of Groundwater Level

The PCA method was used to study quantitatively the impact of climatic and human factors on the groundwater level in Yaoba Oasis in this work. The average rainfall (X_1 , mm), evaporation (X_2 , mm), temperature (X_3 , °C), relative humidity (X_4 , %), irrigated area (X_5 , km²), population (X_6 , number), and exploitation amount (X_7 , million m³) from 1973 to 2018 were used as the original variables, and the annual groundwater level (Y , m) was taken as the dependent variable. The data of influencing factors were normalized, and their correlation coefficient matrix U was calculated as listed in Table 5. Correlation coefficients among the seven variables were high, especially between the exploitation and irrigated area. Hence, the seven variables showed multicollinearity which means the independent principal components need to be extracted in the next work to represent those original variables.

Table 5. Correlation coefficient matrix U of the seven variables from 1973 to 2018.

Factor	X_1	X_2	X_3	X_4	X_5	X_6	X_7
X_1	1	−0.202	−0.098	0.375	−0.143	0.377	−0.106
X_2	−0.202	1	0.282	−0.401	−0.773	−0.377	−0.789
X_3	−0.098	0.282	1	−0.473	−0.226	0.155	−0.244
X_4	0.375	−0.401	−0.473	1	0.139	−0.131	0.147
X_5	−0.143	−0.773	−0.226	0.139	1	0.392	0.921
X_6	0.377	−0.377	0.155	−0.131	0.392	1	0.236
X_7	−0.106	−0.789	−0.244	0.147	0.921	0.236	1

The eigenvalue and contribution rate of U were listed in Table 6. In general, only the eigenvalue greater than 1 could be used as the principal component. As shown in Table 6, the maximum eigenvalue was 3.023, and its contribution rate was 43.189%. The second eigenvalue was 1.573, and its contribution rate was 22.465%. The third eigenvalue was 1.366, and its contribution rate was 19.511%. The cumulative contribution rate of the first three principal components reached 85.164% (>80%) [51]. In other words, three principal components can extract 85.146% of the original information. In addition, the slope of scree plots curve was noticeably slower reaching to the fourth principal component (Figure 10). Thus, the original variable can be replaced by the first three principal components (i.e., Z_1 , Z_2 , and Z_3).

The eigenvectors corresponding to the eigenvalues are listed in Table 7. The principal component linear equation is given as follows:

$$\begin{aligned}
 Z_1 &= 0.190X_1 - 0.534X_2 - 0.368X_3 + 0.207X_4 + 0.429X_5 + 0.148X_6 + 0.015X_7 \\
 Z_2 &= -0.453X_1 + 0.018X_2 + 0.471X_3 - 0.153X_4 + 0.721X_5 + 0.234X_6 + 0.765X_7 \\
 Z_3 &= 0.637X_1 - 0.059X_2 + 0.341X_3 - 0.075X_4 - 0.113X_5 + 0.252X_6 - 0.178X_7
 \end{aligned}
 \tag{3}$$

Table 6. Eigenvalue and contribution rate of U .

Principal Component	Eigenvalue	Initial Eigenvalues		Extraction	Extraction Sums of Squared Loadings		
		Variance Contribution Rate	Cumulative Contribution Rate	Communalities	Principal Eigenvalue	Variance Contribution Rate	Cumulative Contribution Rate
1	3.023	43.189	43.189	0.901	3.023	43.189	43.189
2	1.573	22.465	65.654	0.867	1.573	22.465	65.654
3	1.366	19.511	85.164	0.676	1.366	19.511	85.164
4	0.538	7.690	92.854	0.802			
5	0.295	4.216	97.070	0.950			
6	0.159	2.275	99.345	0.847			
7	0.046	0.655	100	0.921			

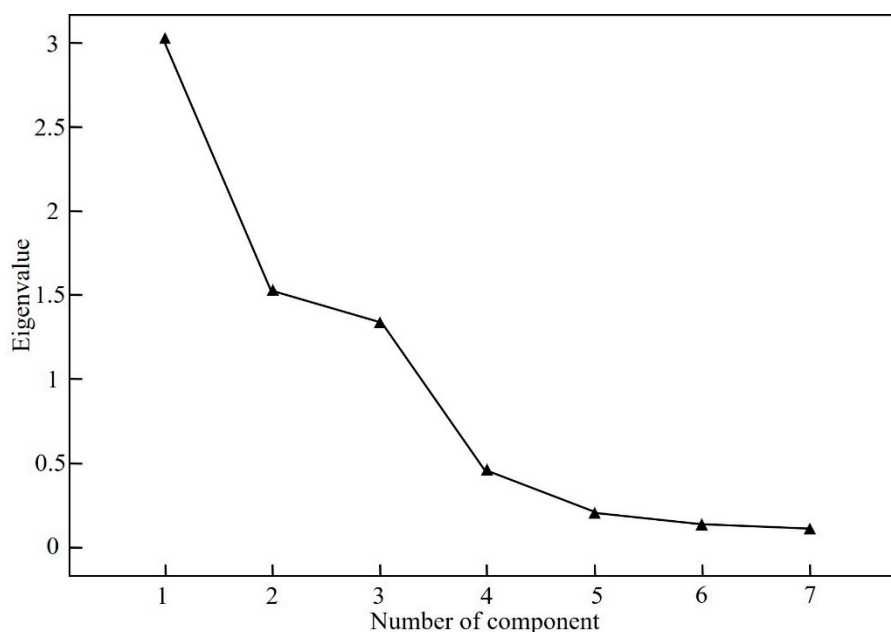


Figure 10. Scree plots map of the eigenvalues in main component.

Table 7. Eigenvector corresponding to the eigenvalue of principal component.

Principal Component	Eigenvector						
	X_1	X_2	X_3	X_4	X_5	X_6	X_7
1	0.190	−0.534	−0.368	0.207	0.429	0.148	0.015
2	−0.453	0.018	0.471	−0.153	0.765	0.234	0.721
3	0.637	−0.059	0.341	−0.075	−0.113	0.252	−0.178

As shown in Table 7, the X_2 (evaporation) had the largest coefficient of 0.534 in the first principal component Z_1 . Hence, the evaporation played a leading role in Z_1 . The first principal component Z_1 was defined as the evaporation climatic factor. The 0.765 coefficient of X_7 (exploitation amount) in the second principal component Z_2 was the largest value. Thus, the exploitation played a leading role in Z_2 . In summary, the second principal component Z_2 was defined as the human factor. The X_1 (rainfall) had the largest coefficient of 0.637 in the third principal component Z_3 . Hence, the rainfall played a leading role in Z_3 . Thus, the third principal component Z_3 was defined as the rainfall climatic factor. As listed in the linear representation of the three principal components (Equation (3)), Z_1 , Z_2 , and Z_3 , which are independent of one another and not collinear, can represent most original variable information. Therefore, multivariable linear regression analysis was performed in the next work.

In accordance with the principle of linear regression, the standardized annual groundwater level Y from 1982 to 2018 was taken as the dependent variable. The evaporation factor Z_1 , human factor Z_2 , and rainfall factor Z_3 were taken as the independent variables. The linear regression equation was obtained by SPSS 25 as follows:

$$Y = -0.166 - 0.090Z_1 - 0.935Z_2 + 0.040Z_3 \quad (4)$$

From Equation (4), the correlation coefficient R and the determination coefficient R^2 were 0.949 and 0.902, respectively. The test value $F = 57.993$, and the probability $P = 0.000 < 0.001$ significance level. On this basis, the regression equation performed well and could effectively quantify climate change and human activities on the impact of groundwater level in Yaoba Oasis. The contribution rate of human factor contributed 87.79%, evaporation factor accounted for 8.45%, and rainfall factor accounted for 3.76% according to the analysis on the relative influence percentage of various factors on

the change in groundwater level. The influence of the human factor on the groundwater level was evidently much greater than that of the climatic factor. The reason was that the climatic factor affected the overall pattern of the ecological environment while the impact on a few areas was not as evident as the human factor. Therefore, the impact of the human factor had a clear indication of the change in groundwater level with the maximum coefficient of exploitation whereas rainfall and evaporation had a certain relatively weak influence on the groundwater level.

The positive and negative signs indicate the positive and negative effects of influencing factors on the groundwater level [44]. From Equation (4), human activities, such as unreasonable mass exploitation, rapid population growth, and gradual expansion of irrigated area, had a strong negative effect on the groundwater level in recent years, which caused a dramatic drop in groundwater level. Although the influence of rainfall on the groundwater level was much fewer than that of human activities, it had the driving force to increase the groundwater level. As a result, the groundwater level of the study area was mainly affected by human and climatic factors. The main influencing factors are exploitation, rainfall, and evaporation. In particular, the exploitation amount, as an important sensitive factor, aggravated the instability of groundwater system and significantly impacted groundwater circulation. In conclusion, affected by the combination of climate change and human activities, the groundwater level in Yaoba Oasis was greatly reduced, and the ecological environment tended to deteriorate.

In future development programs, the depressurization of exploitation amount in groundwater resources is vital for balancing the groundwater system. Feasible solutions, such as shrinkage of the irrigated area, the adjustment of the crop-planting structure, and the generalization of water-saving measures, can effectively reduce the exploitation of groundwater to achieve the sustainable development of the eco-environment, agriculture, and economy in Yaoba Oasis.

4. Conclusions

This study analyzed the annual and inter-annual variation characteristics of groundwater levels from 1982 to 2018 in YaoBa Oasis via Morlet wavelet analysis. The results are as follows: (1) The annual variations of groundwater level contained a spring irrigation decline period from March to May, a summer irrigation decline period from June to August, and an intermittent irrigation recovery period from September to February in the following year. (2) The inter-annual variations of groundwater level were divided into four stages: a slowly dropping period from 1981 to 1997, a rapidly declining period from 1997 to 2004, a slowly declining period from 2004 to 2008, and a stable period from 2008 to 2018. (3) The periodic evolution process of monthly groundwater level occurs in two time scales of 7–15 and 17–35 months, and the first main periodicity is 12 months. (4) The cone of depression experienced emergence, expansion, and reduction periods. The area of the cone of depression first expanded from 1.13 km² in 1985 to 27.16 km² in 2008 and minimized to 11.26 km² in 2018 due to the water-saving measures after 2009.

The MK test and linear trend method were also used to identify the variation trend of influencing factors in groundwater level. In accordance with the change in climatic factors from 1954 to 2018 in the study area, the temperature showed a significant upward trend, which was consistent with the global warming trend. Furthermore, the rainfall increased slightly, and the evaporation and relative humidity showed an insignificant downward trend. In the past 60 years, human activities, such as exploitation and irrigated areas, had intensified the utilization of groundwater resources in the oasis. Therefore, as a qualitative result, the combination of climatic factors and human activities caused a significant drop in groundwater level.

Moreover, PCA was further proposed to quantify the contribution percentage of climate change and human activities to the groundwater level changes. The calculation showed that human factors accounted for 87.79%, whereas climatic factors contributed 12.21%. Accordingly, the overall variation in groundwater level could be attributed to human activities, which outpaced the impacts of climate change. Thus, exploitation amount could be considered a major factor influencing the characteristics

of groundwater level. In summary, the groundwater level dropped as exploitation increased in Yaoba Oasis.

Not only were the temporal and spatial variation characteristics of groundwater levels in a typical oasis in the arid northwest region of China realized, but the influencing degree of climate change and human activity response to groundwater was also quantified in this study. The research results can guide scientific groundwater exploitation planning and management for sustainable development of the oasis and provide novel ideas for similar research in other similar arid oases.

Author Contributions: H.L. and Y.L. were responsible for the original concept and writing the paper. C.Z. and X.Z. processed the data and conducted the program design. B.Z. and J.W. revised the manuscript and shared numerous comments and suggestions to improve the study quality. All authors have read and agreed to the published version of the manuscript.

Funding: This research was supported by the National Natural Science Foundation of China (Nos. 41630634 and 41877179), the General Program of Qinghai Province (No. 2017-ZJ-909), and the Fundamental Research Funds for the Central Universities, CHD (No. 300102290719).

Acknowledgments: The local government and the hydrographic bureau in the Alxa Left Banner of China are greatly appreciated for providing the monitoring data of hydrology and meteorology and their helpful suggestions concerning the manuscript. The authors are grateful to the editor and reviewers for providing positive and constructive comments for this paper.

Conflicts of Interest: The authors declare no conflict of interest.

References

1. Wada, Y.; van Beek, L.P.H.; van Kempen, C.M.; Reckman, J.W.T.M.; Vasak, S.; Bierkens, M.F.P. Global depletion of groundwater resources. *Geophys. Res. Lett.* **2010**, *37*, L20402. [[CrossRef](#)]
2. Viviana, R.E. Groundwater Management in Arid and Semi-Arid Regions: Challenges and Opportunities. In Proceedings of the 3rd National Meeting on Hydrogeology, Cagliari, Italy, 14–16 June 2017.
3. Rohde, M.M.; Froend, R.; Howard, J. A Global Synthesis of Managing Groundwater Dependent Ecosystems under Sustainable Groundwater Policy. *Groundwater* **2017**, *55*, 293–301. [[CrossRef](#)] [[PubMed](#)]
4. Xu, X.; Huang, G.; Sun, C.; Pereira, L.S.; Ramos, T.B.; Huang, Q.; Hao, Y. Assessing the effects of water table depth on water use, soil salinity and wheat yield: Searching for a target depth for irrigated areas in the upper yellow river basin. *Agric. Water Manag.* **2013**, *125*, 46–60. [[CrossRef](#)]
5. Xu, W.; Su, X.S. Challenges and impacts of climate change and human activities on groundwater-dependent ecosystems in arid areas—A case study of the Nalenggele alluvial fan in NW China. *J. Hydrol.* **2019**, *573*, 376–385. [[CrossRef](#)]
6. Skrzypek, G.; Dogramaci, S.; Rouillard, A.; Grierson, P.F. Groundwater seepage controls salinity in a hydrologically terminal basin of semi-arid northwest Australia. *J. Hydrol.* **2016**, *542*, 627–636. [[CrossRef](#)]
7. Alfarrach, N.; Walraevens, K. Groundwater Overexploitation and Seawater Intrusion in Coastal Areas of Arid and Semi-Arid Regions. *Water* **2018**, *10*, 143. [[CrossRef](#)]
8. Keilholz, P.; Disse, M.; Halik, Ü. Effects of land use and climate change on groundwater and ecosystems at the middle reaches of the Tarim River using the MIKE SHE integrated hydrological model. *Water* **2015**, *7*, 3040–3056. [[CrossRef](#)]
9. Abliz, A.; Tiyip, T.; Ghulam, A.; Halik, Ü.; Ding, J.L.; Sawut, M.; Zhang, F.; Nurmemet, I.; Abliz, A. Effects of shallow groundwater table and salinity on soil salt dynamics in the Keriya oasis, northwestern China. *Environ. Earth Sci.* **2016**, *75*, 260. [[CrossRef](#)]
10. Hao, Y.Y.; Xie, Y.W.; Ma, J.H.; Zhang, W.P. The critical role of local policy effects in arid watershed groundwater resources sustainability: A case study in the Minqin oasis, China. *Sci. Total Environ.* **2017**, *601*, 1084–1096. [[CrossRef](#)]
11. Rodell, M.; Velicogna, I.; Famiglietti, J.S. Satellite-based estimates of groundwater depletion in India. *Nature* **2009**, *460*, 999–1002. [[CrossRef](#)]
12. Tweed, S.; Leblanc, M.; Cartwright, I.; Favreau, G.; Leduc, C. Arid zone groundwater recharge and salinization processes; an example from the Lake Eyre Basin, Australia. *J. Hydrol.* **2011**, *408*, 257–275. [[CrossRef](#)]
13. Konikow, L.F. Long-term groundwater depletion in the United States. *Groundwater* **2014**, *53*, 2–9. [[CrossRef](#)] [[PubMed](#)]

14. Powell, O.; Fensham, R. The history and fate of the Nubian Sandstone Aquifer springs in the oasis depressions of the Western Desert, Egypt. *Hydrol. J.* **2015**, *24*, 395–406. [[CrossRef](#)]
15. Alcalá, F.J.; Martínez-Valderrama, J.; Robles-Marín, P.; Guerrero, F.; Martín-Martín, M.; Raaelli, G.; DeLeón, J.T.; Asebriy, L. A hydrological-economic model for sustainable groundwater use in sparse-data drylands: Application to the amtoudi oasis in southern Morocco, northern Sahara. *Sci. Total Environ.* **2015**, *537*, 309–322. [[CrossRef](#)]
16. Zhang, M.; Luo, G.; Hamdi, R.; Qiu, Y.; Wang, X.; Maeyer, P.D.; Kurban, A. Numerical simulations of the impacts of mountain on oasis effects in arid Central Asia. *Atmosphere* **2017**, *8*, 212. [[CrossRef](#)]
17. Ali, R.; McFarlane, D.; Varma, S.; Dawes, W.; Emelyanova, I.; Hodgson, G.; Charles, S. Potential climate change impacts on groundwater resources of south-western Australia. *J. Hydrol.* **2012**, *475*, 456–472. [[CrossRef](#)]
18. Taylor, R.G.; Scanlon, B.; Döll, P.; Rodell, M.; Beek, R.V.; Wada, Y.; Longueuevigne, L.; Leblanc, M.; Famiglietti, J.; Edmunds, M.; et al. Ground water and climate change. *Nat. Clim. Chang.* **2012**, *3*, 322–329. [[CrossRef](#)]
19. Ma, J.Z.; Wang, X.S.; Edmunds, W.M. The characteristics of ground-water resources and their changes under the impacts of human activity in the arid Northwest China—a case study of the Shiyang River Basin. *J. Arid Environ.* **2005**, *61*, 277–295. [[CrossRef](#)]
20. Khan, H.H.; Khan, A.; Ahmed, S.; Perrin, J. GIS-based impact assessment of land-use changes on groundwater quality: Study from a rapidly urbanizing region of South India. *Environ. Earth Sci.* **2010**, *63*, 1289–1302. [[CrossRef](#)]
21. Russo, T.A.; Lall, U. Depletion and response of deep groundwater to climate-induced pumping variability. *Nat. Geosci.* **2017**, *10*, 105–108. [[CrossRef](#)]
22. Malekinezhad, H.; Banadkooki, F.B. Modeling impacts of climate change and human activities on groundwater resources using MODFLOW. *J. Water Clim. Chang.* **2017**, *9*, 156–177. [[CrossRef](#)]
23. Wang, W.K.; Zhang, Z.Y.; Duan, L.; Wang, Z.F.; Zhao, Y.Q.; Dei, M.L.; Liu, H.Z.; Zheng, X.Y.; Sun, Y.B. Response of the groundwater system in the Guanzhong Basin (central China) to climate change and human activities. *Hydrogeol. J.* **2018**, *26*, 1429–1441. [[CrossRef](#)]
24. Feng, D.P.; Zheng, Y.; Mao, Y.X.; Zhang, A.J.; Wu, B.; Li, J.G.; Tian, Y.; Wu, X. An integrated hydrological modeling approach for detection and attribution of climatic and human impacts on coastal water resources. *J. Hydrol.* **2018**, *557*, 305–320. [[CrossRef](#)]
25. Zheng, C.; Lu, Y.D.; Guo, X.H.; Li, H.H.; Sai, J.M.; Liu, X.H. Application of HYDRUS-1D model for research on irrigation infiltration characteristics in arid oasis of northwest China. *Environ. Earth Sci.* **2017**, *76*, 785. [[CrossRef](#)]
26. Li, X.G.; Xia, W.; Lu, Y.D. Optimising the allocation of groundwater carrying capacity in a data-scarce region. *Water SA* **2010**, *36*, 451–460. [[CrossRef](#)]
27. Cui, G.Q.; Lu, Y.D.; Zheng, C.; Liu, Z.H.; Sai, J.M. Relationship between soil salinization and groundwater hydration in Yaoba Oasis, Northwest China. *Water* **2019**, *11*, 175. [[CrossRef](#)]
28. Mann, H.B. Non parametric tests against trend. *Econ. Trica* **1945**, *13*, 245–259.
29. Kendall, M.G. *Rank Correlation Methods*; Charles Griffin: London, UK, 1975.
30. Lacombe, G.; McCartney, M.; Forkuor, G. Drying climate in Ghana over the period 1960–2005: Evidence from the resampling-based Mann–Kendall test at local and regional levels. *Hydrol. Sci. J.* **2012**, *57*, 1594–1609. [[CrossRef](#)]
31. Polemio, M.; Lonigro, T. Trends in climate, short-duration rainfall, and damaging hydrogeological events (Apulia, Southern Italy). *Nat. Hazards* **2015**, *75*, 515–540. [[CrossRef](#)]
32. Chowdhury, R.K.; Beecham, S.; Boland, J.; Piantadosi, J. Understanding South Australian rainfall trends and step changes. *Int. J. Climatol.* **2015**, *35*, 348–360. [[CrossRef](#)]
33. Wu, H.; Qian, H. Innovative trend analysis of annual and seasonal rainfall and extreme values in Shaanxi, China, since the 1950s. *Int. J. Climatol.* **2016**, *37*, 2582–2592. [[CrossRef](#)]
34. Hamed, K.H. Trend detection in hydrologic data: The Mann–Kendall trend test under the scaling hypothesis. *J. Hydrol.* **2008**, *349*, 350–363. [[CrossRef](#)]
35. Jia, Z.X.; Zang, H.F.; Zheng, X.Q.; Xu, Y.X. Climate change and its influence on the karst groundwater recharge in the Jinci Spring Region, Northern China. *Water* **2017**, *9*, 267. [[CrossRef](#)]
36. Coulibaly, P.; Burn, D.H. Wavelet analysis of variability in annual Canadian streamflows. *Water Resour. Res.* **2004**, *40*, W03105.1–W03105.14. [[CrossRef](#)]

37. Partal, T. Wavelet analysis and multi-scale characteristics of the runoff and precipitation series of the Aegean region (Turkey). *Int. J. Climatol.* **2010**, *32*, 108–120. [[CrossRef](#)]
38. Adamowski, J.; Chan, H.F. A wavelet neural network conjunction model for groundwater level forecasting. *J. Hydrol.* **2011**, *407*, 28–40. [[CrossRef](#)]
39. Khalil, B.; Broda, S.; Adamowski, J.; Ozga-Zielinski, B.; Donohoe, A. Short-term forecasting of groundwater levels under conditions of mine-tailings recharge using wavelet ensemble neural network models. *Hydrogeol. J.* **2014**, *23*, 121–141. [[CrossRef](#)]
40. Nourani, V.; Mehr, A.D.; Azad, N. Trend analysis of hydroclimatological variables in Urmia lake basin using hybrid wavelet Mann–Kendall and Şen tests. *Environ. Earth Sci.* **2018**, *77*, 207. [[CrossRef](#)]
41. Mencio, A.; Mas-Pla, J. Assessment by multivariate analysis of groundwater-surface water interactions in urbanized Mediterranean streams. *J. Hydrol.* **2008**, *352*, 355–366. [[CrossRef](#)]
42. Cloutier, V.; Lefebvre, R.; Therrien, R.; Savard, M.M. Multivariate statistical analysis of geochemical data as indicative of the hydrogeochemical evolution of groundwater in a sedimentary rock aquifer system. *J. Hydrol.* **2008**, *353*, 294–313. [[CrossRef](#)]
43. Gangopadhyay, S.; Das Gupta, A.; Nachabe, M.H. Evaluation of ground water monitoring network by principal component analysis. *Ground Water* **2001**, *39*, 181–191. [[CrossRef](#)] [[PubMed](#)]
44. Halim, M.A.; Majumder, R.K.; Nessa, S.A.; Oda, K.; Hiroshiro, Y.; Jinno, K. Arsenic in shallow aquifer in the eastern region of Bangladesh: Insights from principal component analysis of groundwater compositions. *Environ. Monit. Assess.* **2010**, *161*, 453–472. [[CrossRef](#)] [[PubMed](#)]
45. Hu, S.; Luo, T.; Jing, C.Y. Principal component analysis of fluoride geochemistry of groundwater in Shanxi and Inner Mongolia, China. *J. Geochem. Explor.* **2013**, *135*, 124–129. [[CrossRef](#)]
46. Li, H.H.; Lu, Y.D.; Zheng, C.; Yang, M.; Li, S.L. Groundwater level prediction for the arid oasis of northwest China based on the artificial bee colony algorithm and a back-propagation neural network with double hidden layers. *Water* **2019**, *11*, 860. [[CrossRef](#)]
47. Li, X.; Lu, Y.D.; Zhang, X.Z.; Zhang, R.; Fan, W.; Pan, W.S. Influencing Factors of the Spatial-Temporal Variation of Layered Soils and Sediments Moistures and Infiltration Characteristics under Irrigation in a Desert Oasis by Deterministic Spatial Interpolation Methods. *Water* **2019**, *11*, 1483. [[CrossRef](#)]
48. Abdalla, O.A.E. Groundwater discharge mechanism in semi-arid regions and the role of evapotranspiration. *Hydrol. Process.* **2008**, *22*, 2993–3009. [[CrossRef](#)]
49. Haj-Amor, Z.; Tóth, T.; Ibrahimi, M.K.; Bouri, S. Effects of excessive irrigation of date palm on soil salinization, shallow groundwater properties, and water use in a Saharan oasis. *Environ. Earth Sci.* **2017**, *76*, 590. [[CrossRef](#)]
50. Zhang, Z.D.; Wan, L.W.; Dong, C.W.; Xie, Y.C.; Yang, C.X. Impacts of climate change and human activities on the surface runoff in the Wuhua River Basin. *Sustainability* **2018**, *10*, 3405. [[CrossRef](#)]
51. Uddameri, V.; Honnunar, V.; Hernandez, E.A. Assessment of groundwater water quality in central and southern Gulf Coast aquifer, TX using principal component analysis. *Environ. Earth Sci.* **2014**, *71*, 2653–2671. [[CrossRef](#)]

